STUDIA UBB CHEMIA, LXX, 2, 2025 (p. 7-18)
(RECOMMENDED CITATION)
DOI:10.24193/subbchem.2025.2.01

INVESTIGATION OF OPTICAL PROPERTIES AND SOLID-STATE STRUCTURE OF THIOPHENE-CONTAINING TRIARYLAMINE DERIVATIVES

Daniel-Florin BOGOȘEL[a], Andreea Petronela CRIȘAN[a], Alexandra POP[a], Anamaria TEREC[a,*], Ion GROSU[a,*]

ABSTRACT. The optoelectronic properties of some thiophene-containing triarylamines derived formally from triphenyl amine by enlarging one, two, or all phenyl groups with phenyl, thiophene-phenyl, bithiophene, or terthiophene units, along with the molecular structure and the supramolecular arrangement of the molecules in the lattices, were revealed by spectroscopic and, in the case of two of the compounds, single crystal X-ray diffractometry investigations. This study confirms that solid-state interactions and conformations significantly influence the absorption and emission characteristics of these compounds, essential factors in designing efficient photovoltaic materials.

Keywords: *triarylamine, absorption and emission spectra, single crystal X-ray diffractometry, C-H···π and heteroatom···π contacts*

INTRODUCTION

Nowadays, our society faces significant challenges regarding the efficient use of current resources alongside the mindful exploitation of renewable energy sources, and finding new functional materials has become one of the most investigated lines of research over the last 25 years. Triphenylamine (TPA) or, more generally, triarylamine (TAA) derivatives distinguished themselves among the electroactive building blocks in functional materials, being used as hole transporters in numerous optoelectronic devices that convert solar light into

[a] *Babes-Bolyai University, Faculty of Chemistry and Chemical Engineering, Department of Chemistry and SOOMCC, Cluj-Napoca, 11 Arany Janos, 400028, Cluj-Napoca, Romania.*
[*] *Corresponding authors: anamaria.terec@ubbcluj.ro; ion.grosu@ubbcluj.ro*

electricity,[1–3] such as organic solar cells (OSCs),[4–6] dye-sensitized solar cells (DSSCs),[7] and perovskite solar cells (PSCs).[8] Some TAA derivatives are luminescent and thus can be used in organic light emitting diodes (OLEDs)[9–11] and organic field effect transistors (OFETs)[12] or act as sensors[13, 14] and electrochromic systems.[15]

TAAs have strong electron-donating capability that allows for the construction of extended π-systems toward acceptor moieties for hole-transporting properties, while the nonplanar propeller-shaped TPA unit restrains intermolecular aggregation via π-π stacking that usually leads to fluorescence quenching in the solid state. In most materials, the solid-state luminescent properties closely follow the intermolecular interactions that occur in aggregates or crystals.

In this context, our attention was directed toward two TAA derivatives containing thiophene units in the conjugated π-system (Chart 1). The supramolecular structure of smaller thiophene-containing TPA aldehydes (**TPA2TfCHO** and **TPA3TfCHO**) (Chart 2) was already reported in the literature [16–19] while the simplest brominated TPA derivative, *p*-bromotriphenylamine (**TPABr**) found application in various functional materials[20, 21] – for example, it was used as an additive in hybrid materials to enhance the fluorescence and phosphorescence of carbazole derivatives via halogen bonding.[22] Thus, we considered it of interest to investigate the luminescent properties of TAAs **1** and **2** in correlation with their supramolecular association in crystals to account for the influence of the extended π-systems on their properties.

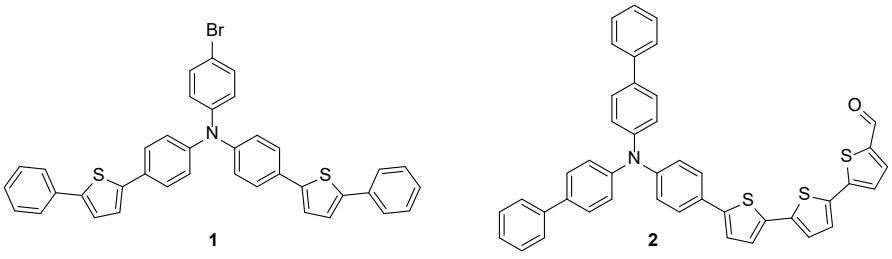

Chart 1

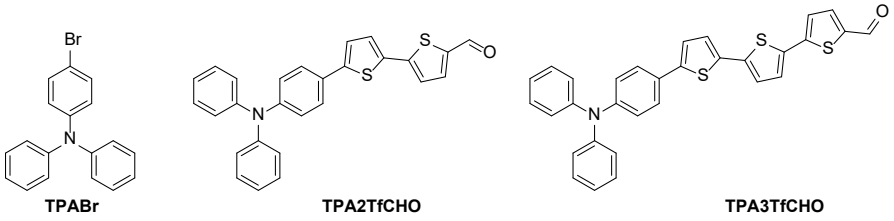

Chart 2

RESULTS AND DISCUSSIONS

We have accessed TAA derivatives **1** and **2** in our laboratory through multi-step synthesis from commercially available materials.[23] Additionally, we have synthesised the already-reported **TPABr**, **TPA2TfCHO,** and **TPA3TfCHO** as reference compounds.

First, the photophysical behaviour of the compounds in solution was examined to assess how structural changes in the extended TAA derivatives affect their optical properties.

The UV-VIS absorption spectra of the compounds were recorded in CH_2Cl_2 (10^{-5} M) and are presented in **Figure 1a**.

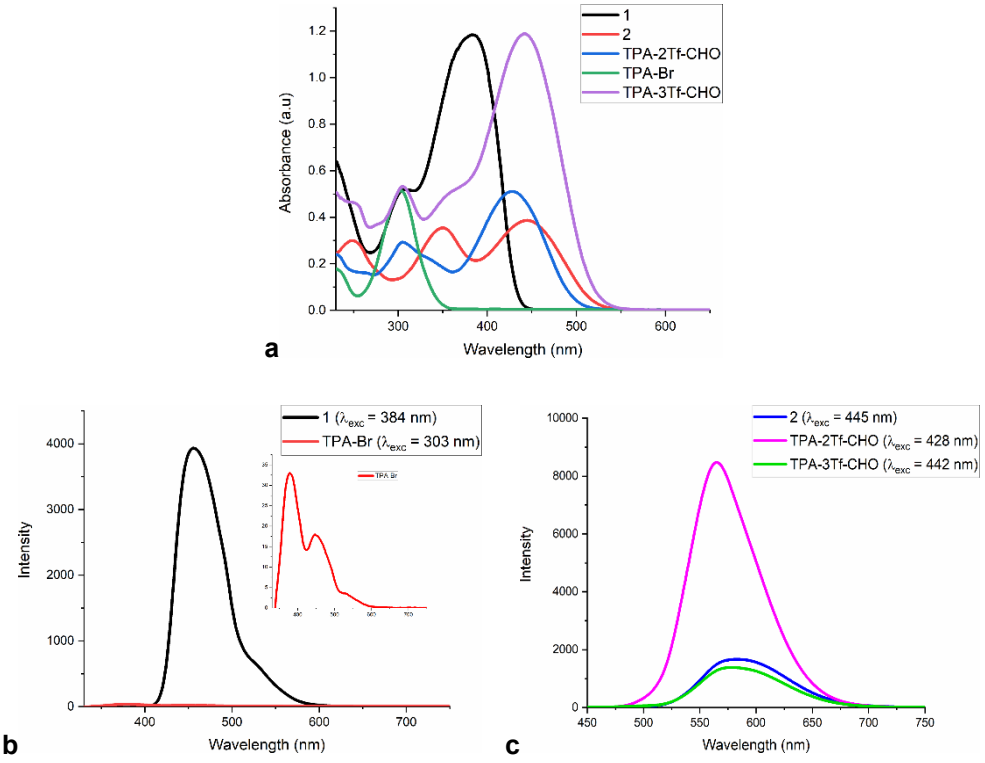

Figure 1. a) UV-vis absorption spectra of compounds **1**, **2**, **TPABr**, **TPA2TfCHO,** and **TPA3TfCHO** in 10^{-5}M CH_2Cl_2 solution; b) Emission spectra of brominated derivatives **1** and **TPABr** in $1.5x10^{-5}$M CH_2Cl_2 solution; c) Emission spectra of aldehydes **2**, **TPA2TfCHO,** and **TPA3TfCHO** in $1.5x10^{-5}$M CH_2Cl_2 solution.

Most of the compounds exhibit first absorption bands in the range of 300-305 nm, corresponding to π-π* transitions in the molecules. Among the studied compounds, a noticeable red-shift of the π-π* absorption band appears for compound **2** at 350 nm, which can be ascribed to the extended conjugation in the system. Additionally, all compounds, except for **TPABr**, exhibit a supplementary peak (at 385 nm for **1** and around 430-450 nm for the aldehydes) that can be associated with internal charge transfer (ICT) due to π-π stacking and transfer from the donor (TAA) to the acceptor (CHO) part of the molecule. The emission characteristics were investigated by recording the fluorescence spectra in $1.5x10^{-5}$ M CH_2Cl_2 solutions (Figure 1 b and c). All compounds, except for TPABr, display fluorescence exhibiting emission with maxima around 450 nm for **1** and red-shifted to 565-585 nm for the aldehydes due to ICT phenomena, confirming the extended π-π conjugation (**Figures 1b and 1c**).

Both our compounds showed only modest optical performances compared to some already reported compounds with similar functionalities used in photovoltaics, for which an increase in the intensities of ICT vs. π-π* transitions was associated with a better conjugation favoured by the near-coplanarity of the extended π system.[24, 25]

To explain these observations, we have investigated their structure in solid state. Yellow crystals of **1** and orange crystals of **2** suitable for Single Crystal X-Ray Diffraction were obtained by slow evaporation of chloroform (**1**) and acetone/dichloromethane/pentane (1/1/1) solutions (**2**), respectively. Their molecular structures are presented in **Figure 2**. As a common feature, both compounds present a quasiplanar central triarylamine unit with (Ar)C-N-C(Ar) bond angles of approximately 120° and the propeller-like arrangement of the aryl groups around the N atom (torsion angles between 50° and 57° for **1** and between 24° and 65° for **2**, respectively).

Contrary to our expectations, the π-conjugated system in **1** strongly deviates from the desired coplanarity, with torsion angles in the range of 5.18° and 29.65° (depicted in blue in **Figure 3a**). This fact has poorer electron delocalization consequences. The unit cell consists of four molecules arranged in an antiparallel manner (**Figure 3a**), and the formation of catemeric chains connected *via* halogen bonds can also be noticed. The length between the bromine atom and C10 and C11 (Br-C10 and Br-C11 distances of 3.291 Å and 3.353 Å, respectively, depicted in red in **Figure 3**) is less than the sum of their Van der Waals radii (3.40 Å)[26], leading to above-the-bond C-Br···π halogen bonding.[27, 28]

The three-dimensional crystal packing of **1** presented in **Figure 3b** shows the formation of antiparallelly running catemers held together by multiple weak intermolecular C-H···π contacts (H31···Cg1 [Cg1 = thiophene (S2) ring] distance of 2.785 Å and H35···Cg2 [Cg2 = C1-C6 phenyl ring]

distance of 3.102 Å) depicted in green. Similar C-H···π contacts were reported previously in some cyclophanes and supramolecular polymers containing fluorene or spirobifluorene units.[29–31]

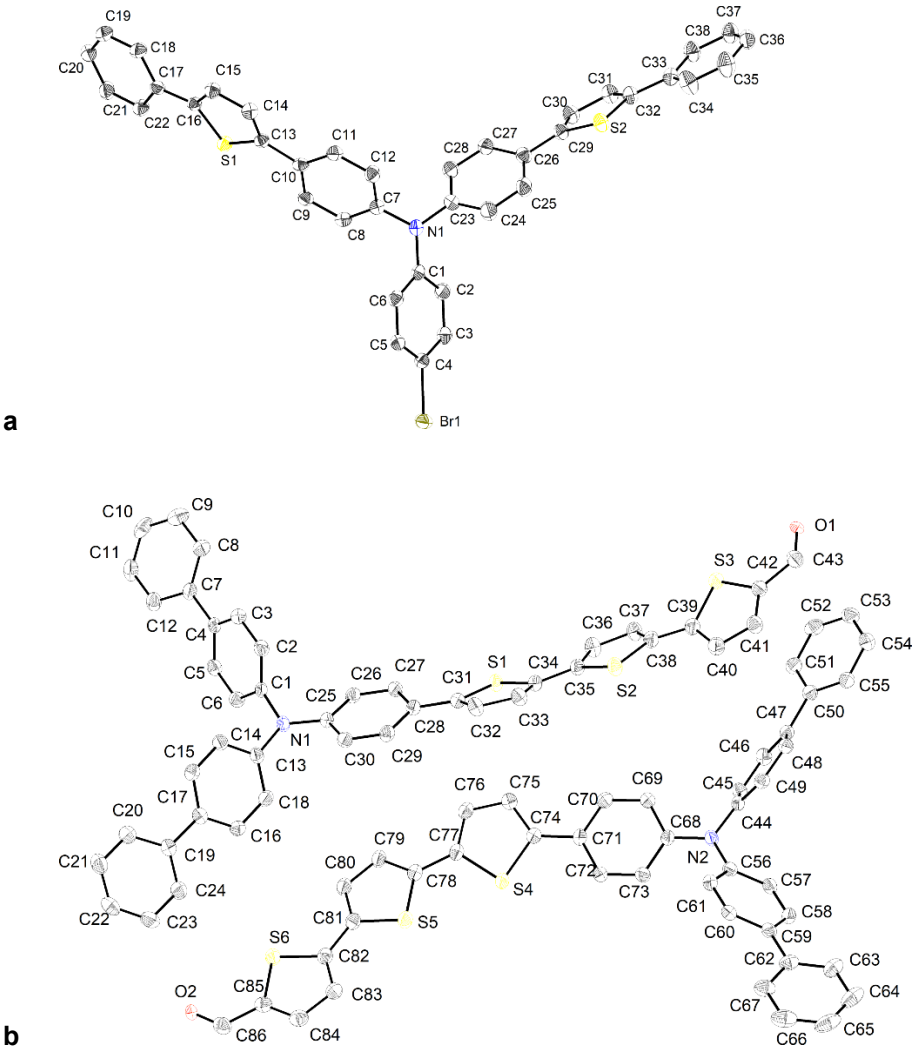

Figure 2. ORTEP representation (50% probability level of atomic displacement ellipsoids) of the molecular structure of compounds **1** (a) and **2** (b). Hydrogen atoms were omitted for clarity

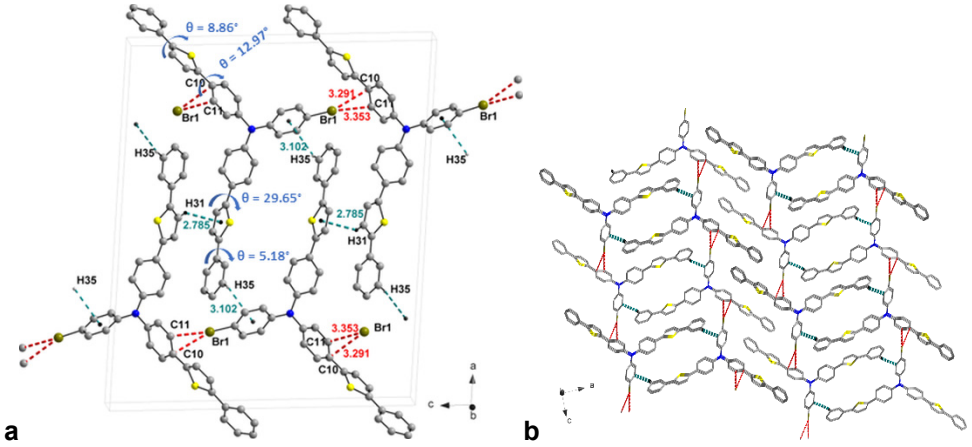

Figure 3. (**a**) Unit cell with detailed intermolecular interactions and significant torsion angles in the π system and (**b**) packing patterns of compound **1** crystal. Hydrogen atoms were omitted for clarity, except when involved in interactions.

The asymmetric unit of compound **2** contains two crystallographically independent molecules (**Figure 4b**) that differ in the relative arrangement of the three thiophene rings. In one of the molecules, there is a *syn-anti* disposal of the thiophene moieties (further named **2SA**), while in the other, the rings adopt an *anti-anti* conformation (further named **2AA**). Similar TAA-containing mono-, di- and terthiophene aldehydes, such as **TPA2TfCHO** and **TPA3TfCHO,** were reported to demonstrate polymorphism under different crystal growth conditions, and, in most reported cases, only same-conformer crystal was observed.[16, 19, 32–34]

Similarly to the above-described brominated triarylamine derivative **1**, there is a significant deviation from coplanarity in the π-conjugated system and, in this case, in the biphenyl terminal units as well. By contrast, in the case of simpler **TPA2TfCHO**, a quasiplanar arrangement of the oligothiophene moiety was observed.[16, 19, 32] In conformer **2AA**, only the middle thiophene units are coplanar with additional stabilization from C-H···S interactions (S2···H33 distance of 2.874 Å and S1···H27 distance of 2.815 Å, depicted in purple in Figure **4a**). Meanwhile, the outer thiophene ring and the connecting phenyl ring jut out at significant angles (θ = 28.40° and θ = 18.95°, respectively, shown in blue in **Figure 4a**). In **2SA** (**Figure 4b**), there is a notable torsion

angle of 20.39° between the two *syn* thiophene rings, while the other aromatic rings in the π system are stabilized in a local near planar conformation by additional C-H···S interactions (S6···H80 distance of 2.915 Å and S4···H72 distance of 2.719 Å, depicted in purple). In both conformers, the biphenyl rings attached to the N atom are twisted at torsion angles ranging from 13.12° to 32.59° (**Figures 4a** and **4b**). We have described similar supramolecular contacts involving the heterocyclic sulphur atoms in solid-state packing of some thiophene- or phenothiazine-containing heterocycles, too.[35, 36]

The conformer **2SA** associates in homomeric dimers (**Figure 4b**) connected in an antiparallel fashion by doubled C-H···O interactions (O2···H52 distance of 2.617 Å, shown in red). The thiophene units directly attached to the phenyl ring are above each other, slightly shifted in parallel planes (3.219 Å distance between planes), and strengthening reciprocal C-H···π interactions are observed (H76···Cg1 [Cg1 = thiophene (S4)] distance is 3.231 Å, depicted in green; Cg1···Cg1 distance 4.150 Å). A somewhat similar situation is encountered in **2AA**, in which dimeric head-to-head formations by C-H···π contacts in the biphenyl units (H11···Cg2 [Cg2 = C13-C18 phenyl] distance of 3.280 Å, depicted in green in **Figure 4a**) are observed, while a neighbouring **2AA** molecule is in an antiparallel arrangement, but more shifted than in **2SA** (2.325 Å distance between the parallel planes with 5.404 Å distance between thiophene (S1) rings centroids).

In turn, the different conformers are associated (**Figure 4c**) through C-H···π contacts (H76···C29 and H76···C28 distances are 2.759 Å and 2.780 Å, respectively, H75···Cg3 [Cg3 = thiophene (S1)] 2.716 Å), and π···π interaction (distance between centroids of thiophene (S3) and phenyl ring is 3.856 Å, depicted in green) alongside C-H···S interactions (S6···H24 distance of 2.847 Å, shown in purple). A plethora of C-H···π intermolecular interactions ranging between 3.092 Å and 3.108 Å (in green in **Figure 4c**) and short C-H···O interactions (O1···H72 distance of 2.392 Å, shown in red) ensures further development of the supramolecular 2D network.

Inspection of the packing diagram of **2** revealed the alternation of homomolecular sheets of connected dimers, as shown in **Figure 4d,** with **2SA** molecules depicted in pink and the **2AA** conformers in green. The deviation from the planarity in both the extended π-system and in the biphenyl part disrupts the effective electron conjugation and constrains the molecules further from each other in the crystalline lattice.

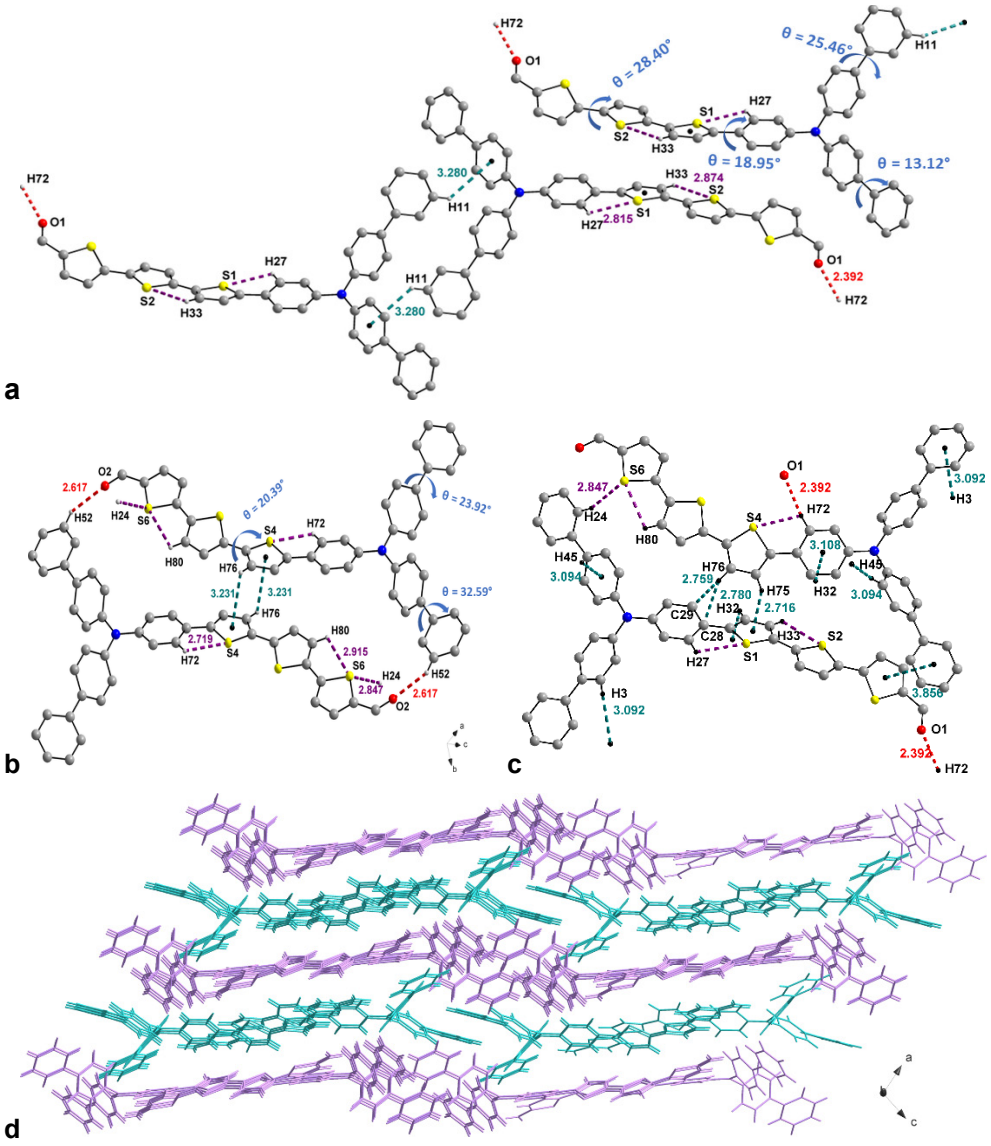

Figure 4. Views of (**a**) **2AA** conformer homomeric association, (b) one **2SA** homomeric dimer formation, (**c**) heteromeric association of **2SA** and **2AA** conformers, and (**d**) packing patterns of compound **2** in crystal showing homomeric (**2SA** conformers are presented in pink and **2AA** ones in green) sheet formation. C-H···π and π···π (depicted in green), C-H···O (in red), and C-H···S (in purple) interactions are shown. Hydrogen atoms were omitted for clarity, except when involved in interactions.

CONCLUSIONS

The absorption spectra of compounds **1** and **2** revealed a bathochromic shift of absorption maxima comparatively to those of TPA compounds with less extended π-π structure. In both absorption and emission spectra, red-shifted peaks belonging to ICT (internal charge transfer) processes were observed. The single crystal X-ray diffractometry investigation of **1** and **2** highlighted the non-planar structure of the di-, ter- or quarter-aryl chains and the association of the molecules in the lattices via C-H···π and heteroatom·π contacts. In conclusion, in the depicted compounds **1** and **2**, the introduction of a more complex and extended π-system brings supplemental intermolecular interactions with detrimental effects on the solid-state packing, an essential feature for functional materials used in photovoltaics. This study underscores the importance of understanding the relationship between molecular structure, solid-state packing, and optical properties in the development of functional materials for electronic applications.

EXPERIMENTAL SECTION

UV-vis optical data in solution were recorded with an UV-vis 1900 Shimadzu spectrometer. Fluorescence spectra were recorded on a JASCO FP-8300 spectrofluorometer using quartz cuvettes (1 cm). Solutions for UV-vis and fluorescence measurements were prepared in HPLC grade dichloromethane.

Details about the crystal structure determination and refinement data are given in **Table S1**. The crystals of **1** and **2** were mounted on MiTeGen microMounts cryoloops, and data were collected on a Bruker D8 VENTURE diffractometer using Mo-Kα radiation (λ = 0.71073 Å) from a IμS 3.0 microfocus source with multilayer optics, at 100 K. The structures were refined with anisotropic thermal parameters for non-H atoms. Hydrogen atoms were placed in fixed, idealized positions and refined with a riding model and a mutual isotropic thermal parameter. For structure solving and refinement the Bruker APEX4 Software Package was used.[37] One solvent molecule in the structure of **1** was found to be disordered over several positions. The SQUEEZE procedure of the PLATON program was used for the removal of the contribution of the electron density from the intensity data corresponding to the disordered solvent. The solvent-free model was employed for the final refinement, and it was estimated that a volume of 274 $Å^3$ corresponds to the pentane used for chromatographic purification.[23, 38] Drawings were created using the Diamond program.[39] The CCDC reference numbers are 2435059 (**1**) and

2435058 (**2**). The supplementary crystallographic data for this article can be obtained free of charge from The Cambridge Crystallographic Data Centre via https://www.ccdc.cam.ac.uk/structures/.

Table S1. Crystal data and structure refinement for **1** and **2**

Compound	**1**	**2**
Molecular formula	$C_{38}H_{26}BrNS_2$	$C_{43}H_{29}NOS_3$
Formula weight	640.63	671.85
Crystal size / mm^3	0.074 x 0.093 x 0.135	0.036 x 0.118 x 0.123
Crystal habit	yellow block	orange-yellow plate
λ(MoK_α) / Å	0.71073	0.71073
T / K	100.(2)	99.(2)
Crystal system	monoclinic	triclinic
Space group	*P21/c*	*P-1*
a / Å	26.0625(9)	10.4861(4)
b / Å	5.5687(2)	13.5328(6)
c / Å	21.6895(8)	23.9078(11)
α / °	90	93.213(2)
β / °	94.1290(10)	102.3010(10)
γ / °	90	98.9090(10)
V / Å^3	3139.72(19)	3260.8(2)
Z	4	4
D_{calc} / g cm^{-3}	1.355	1.369
μ / mm^{-1}	1.470	0.265
θ range for data collections (°)	1.99 - 28.41	2.01 - 28.29
F(000)	1312	1400
T_{max} / T_{min}	0.83 / 0.90	0.96 / 0.99
Refl. collected / unique / R_{int}	95985 / 0.0776	100602 / 0.1021
Completeness to θ	99.8%	99.9%
Refinement method	Full-matrix least-squares on F^2	
Data / restraints / parameters	7875 / 0 / 379	16157 / 0 / 865
Goodness-of-fit, S	0.841	0.993
Final R indices [I>2σ(I)]	R_1 = 0.0472	R_1 = 0.0545
	wR_2 = 0.1743	wR_2 = 0.1380
R indices (all data)	R_1 = 0.0697	R_1 = 0.1051
	wR_2 = 0.2090	wR_2 = 0.1721
$\Delta\rho_{max}$, $\Delta\rho_{min}$ / e Å^{-3}	0.552/ -0.903	0.330 / -0.433
CCDC No.	**2435059**	**2435058**

ACKNOWLEDGEMENTS

This work was supported by the Romanian Ministry of Research, Innovation and Digitization, CNCS – UEFISCDI, research projects PN-III-P4-ID-PCE-2020-1812 (ICOFCOSC), PN-III-P2-2.1-PED-2019-2601 (REGRENPOS) and 312-COFFEE ERANET within PNCDI IV.

REFERENCES

1. R. Rybakiewicz; M. Zagorska; A. Pron; *Chem. Pap.* **2017**, *71* (*2*), 243–268
2. P. Blanchard; C. Malacrida; C. Cabanetos; J. Roncali; S. Ludwigs; *Polym. Int.* **2019**, *68* (*4*), 589–606
3. J. Wang; K. Liu; L. Ma; X. Zhan; *Chem. Rev.* **2016**, *116* (*23*), 14675–14725
4. J. Roncali; P. Leriche; P. Blanchard; *Adv. Mater.* **2014**, *26* (*23*), 3821–3838
5. A. Diac; D. Demeter; M. Allain; I. Grosu; J. Roncali; *Chem. – Eur. J.* **2015**, *21* (*4*), 1598–1608
6. D. Demeter; S. Mohamed; A. Diac; I. Grosu; J. Roncali; *ChemSusChem*. **2014**, *7* (*4*), 1046–1050
7. A. Mahmood; *Sol. Energy*. **2016**, *123*, 127–144
8. P. Agarwala; D. Kabra; *J. Mater. Chem. A*. **2017**, *5* (*4*), 1348–1373
9. J. Kwak; W. K. Bae; M. Zorn; H. Woo; H. Yoon; J. Lim; S. W. Kang; S. Weber; H.-J. Butt; R. Zentel; et al.; *Adv. Mater.* **2009**, *21* (*48*), 5022–5026
10. J.-X. Liang; Z.-H. Pan; K. Zhang; D. Yang; J.-W. Tai; C.-K. Wang; M.-K. Fung; D. Ma; J. Fan; *Chem. Eng. J.* **2023**, *457*, 141074
11. Q. Zhang; J. Jiang; Z. Xu; D. Song; B. Qiao; S. Zhao; S. Wageh; A. Al-Ghamdi; *RSC Adv.* **2021**, *11* (*39*), 24436–24442
12. L. M. Nhari; R. M. El-Shishtawy; A. M. Asiri; *Dyes Pigments*. **2021**, *193*, 109465
13. H. E. Okda; S. E. Sayed; R. C. M. Ferreira; R. C. R. Gonçalves; S. P. G. Costa; M. M. M. Raposo; R. Martínez-Máñez; F. Sancenón; *New J. Chem.* **2019**, *43* (*19*), 7393–7402
14. H. Chen; P. Yang; Y. Li; L. Zhang; F. Ding; X. He; J. Shen; *Spectrochim. Acta. A. Mol. Biomol. Spectrosc.* **2020**, *224*, 117384
15. T. Harimoto; Y. Ishigaki; *Chem. – Eur. J.* **2025**, *31* (*3*), e202403273
16. A. Benitz; M. B. Thomas; Y. Jang; V. Nesterov; F. D'Souza; *J. Chem. Sci.* **2021**, *133* (*3*), 71
17. B. Lv; Z. Wang; Y. Wu; Y. Zheng; Z. Cui; J. Li; W. Gu; *J. Hazard. Mater.* **2024**, *469*, 134105
18. V. Parthasarathy; S. Fery-Forgues; E. Campioli; G. Recher; F. Terenziani; M. Blanchard-Desce; *Small*. **2011**, *7* (*22*), 3219–3229
19. K. Amro; J. Daniel; G. Clermont; T. Bsaibess; M. Pucheault; E. Genin; M. Vaultier; M. Blanchard-Desce; *Tetrahedron*. **2014**, *70* (*10*), 1903–1909

20. A. J. Sindt; B. A. DeHaven; R. L. Goodlett; J. O. Hartel; P. J. Ayare; Y. Du; M. D. Smith; A. K. Mehta; A. M. Brugh; M. D. E. Forbes; C. R. Bowers; A. K. Vannucci; L. S. Shimizu; *J. Am. Chem. Soc.* **2020**, *142* (*1*), 502–511
21. J. Yang; X. Wu; J. Shi; B. Tong; Y. Lei; Z. Cai; Y. Dong; *Adv. Funct. Mater.* **2021**, *31* (*52*), 2108072
22. W. Dai; X. Niu; X. Wu; Y. Ren; Y. Zhang; G. Li; H. Su; Y. Lei; J. Xiao; J. Shi; B. Tong; Z. Cai; Y. Dong; *Angew. Chem. Int. Ed.* **2022**, *61* (*13*), e202200236
23. D.-F. Bogoșel; G.-I. Giurgi; A. Balan; A. Pop; I. Grosu; A. P. Crișan; A. Terec; *Org. Electron.* **2025**, *141*, 107212
24. S. Noureen; P. Devibala; P. M. Imran; S. Nagarajan; *Synth. Met.* **2024**, *302*, 117541
25. N. Terenti; G.-I. Giurgi; A. P. Crişan; C. Anghel; A. Bogdan; A. Pop; I. Stroia; A. Terec; L. Szolga; I. Grosu; J. Roncali; *J. Mater. Chem. C*. **2022**, *10* (*14*), 5716–5726
26. A. Bondi; *J. Phys. Chem.* **1964**, *68* (*3*), 441–451
27. F. C. Grozema; R. W. J. Zijlstra; M. Swart; P. Th. van Duijnen; *Int. J. Quantum Chem.* **1999**, *75* (*4–5*), 709–723
28. Q. J. Shen; X. Pang; X. R. Zhao; H. Y. Gao; H.-L. Sun; W. J. Jin; *CrystEngComm*. **2012**, *14* (*15*), 5027-5034
29. M. Balog; I. Grosu; G. Plé; Y. Ramondenc; E. Condamine; R. A. Varga; *J. Org. Chem.* **2004**, *69* (*4*), 1337–1345
30. I. G. Grosu; L. Pop; M. Miclăuş; N. D. Hădade; A. Terec; A. Bende; C. Socaci; M. Bărboiu; I. Grosu; *Cryst. Growth Des.* **2020**, *20* (*5*), 3429–3441
31. L. Pop; I. G. Grosu; M. Miclăuş; N. D. Hădade; A. Pop; A. Bende; A. Terec; M. Bărboiu; I. Grosu; *Cryst. Growth Des.* **2021**, *21* (*2*), 1045–1054
32. A. Vinod Kumar; P. Pattanayak; A. Khapre; A. Nandi; P. Purkayastha; R. Chandrasekar; *Angew. Chem. Int. Ed.* **2024**, *63* (*40*), e202411054
33. W. Xu; M. M. S. Lee; Z. Zhang; H. H. Y. Sung; I. D. Williams; R. T. K. Kwok; J. W. Y. Lam; D. Wang; B. Z. Tang; *Chem. Sci.* **2019**, *10* (*12*), 3494–3501
34. A. M. Raynor; A. Gupta; C. M. Plummer; S. L. Jackson; A. Bilic; H. Patil; P. Sonar; S. V. Bhosale; *Molecules*. **2015**, *20* (*12*), 21787–21801
35. A. Bende; I. Grosu; I. Turcu; *J. Phys. Chem. A*. **2010**, *114* (*47*), 12479–12489
36. M. Cîrcu; V. Paşcanu; A. Soran; B. Braun; A. Terec; C. Socaci; I. Grosu; *CrystEngComm*. **2012**, *14* (*2*), 632–639
37. G. M. Sheldrick; *Acta Crystallogr. Sect. C Struct. Chem.* **2015**, *71* (*1*), 3–8
38. A. L. Spek; *J. Appl. Crystallogr.* **2003**, *36* (*1*), 7–13
39. DIAMOND – Visual Crystal Structure Information System, **2001**